HHS Public Access

Author manuscript

Anal Bioanal Chem. Author manuscript; available in PMC 2023 May 01.

Published in final edited form as:

Anal Bioanal Chem. 2022 May ; 414(13): 3945–3958. doi:10.1007/s00216-022-04038-y.

MIMAS: Microfluidic Platform in Tandem with MALDI Mass Spectrometry for Protein Quantification from Small Cell Ensembles

Jorvani Cruz Villarreal[1,2], **Rory Kruithoff**[3], **Ana Egatz-Gomez**[1,2], **Paul D. Coleman**[4], **Robert Ros**[3,5], **Todd R. Sandrin**[6,7], **Alexandra Ros**[1,2]

[1]School of Molecular Sciences, Arizona State University, USA

[2]Center for Applied Structural Discovery, The Biodesign Institute, Arizona State University, USA

[3]Department of Physics and Center for Biological Physics, Arizona State University, USA

[4]Banner ASU Neurodegenerative Research Center, The Biodesign Institute, Arizona State University, USA

[5]Center for Single Molecule Biophysics, The Biodesign Institute, Arizona State University, USA

[6]School of Mathematical and Natural Sciences, Arizona State University, USA

[7]Julie Ann Wrigley Global Futures Laboratory, Arizona State University, USA

Abstract

Understanding cell-to-cell variation at the molecular level provides relevant information about biological phenomena and is critical for clinical and biological research. Proteins carry important information not available from single-cell genomics and transcriptomics studies; however, due to the minute amount of proteins in single cells and the complexity of the proteome, quantitative protein analysis at the single cell level remains challenging. Here, we report an integrated microfluidic platform in tandem with matrix-assisted laser desorption ionization time-of-flight mass spectrometry (MALDI-TOF-MS) for the detection and quantification of targeted proteins from small cell ensembles (> 10 cells). All necessary steps for the assay are integrated on-chip including cell lysis, protein immunocapture, tryptic digestion and co-crystallization with the matrix solution for MALDI-MS analysis. We demonstrate that our approach is suitable for protein quantification by assessing the apoptotic protein Bcl-2 released from MCF-7 breast cancer cells, ranging from 26 to 223 cells lysed on-chip (8.75 nL wells). A limit of detection (LOD) of 11.22 nM was determined, equivalent to 5.91×10^7 protein molecules per well. Additionally, the microfluidic platform design was further improved, establishing the successful quantification of Bcl-2 protein from MCF-7 cell ensembles ranging from 8 to 19 cells in 4 nL wells. The LOD in the smaller well designs for Bcl-2 resulted in 14.85 nM, equivalent to 3.57×10^7 protein molecules per well. This work shows the capability of our approach to quantitatively assess proteins from cell lysate on the MIMAS platform for the first time. These results demonstrate

Corresponding Author: Alexandra Ros, Alexandra.Ros@asu.edu, Phone: +1-480-965-5323, Fax: +1-480-965-2757.

CONFLICT OF INTEREST

The authors declare no competing interests.

our approach constitutes a promising tool for quantitative targeted protein analysis from small cell ensembles down to single cells, with the capability for multiplexing through parallelization and automation.

Keywords

Microfluidics; microfabrication; protein; quantification; mass spectrometry

INTRODUCTION

Unlocking cellular heterogeneity on the molecular level is relevant for biological phenomena.[1] Because proteins are key effectors and regulators in cells, understanding their quantitative cell-to-cell variation is of high importance. Assessing proteins allows attainment of information not accessible through single-cell genomic and transcriptomic data such as protein abundance, post-translational modifications (PTMs), isoforms, and protein-protein interactions.[2,3] PTMs, for example, occur during or after the protein biosynthesis, altering protein functionality. Identifying PTMs is of particular interest for unraveling details in protein function related to diseases such as cancer[4], diabetes[5] and neurodegenerative disorders[6]. Thus, understanding protein expression at the single-cell level is important in clinical and biological research; however, due to the minute amount of each specific protein in a single cell (about 10^5-10^6 copies per specific protein in mammalian cells to as low as 50 copies for low abundance proteins)[7] and the complexity of the proteome, quantitative protein analysis in specific subpopulations down to the single cell level remains challenging.

Mass spectrometry (MS) is the workhorse technology for proteomics analysis.[8,9] Achievable detection limits down to sub-attomole to zeptomole ranges[10] make it a powerful tool for single-cell proteomics. Flow or mass cytometry and fluorescence-based detection are other frequently used techniques in single-cell protein analysis. However, limitations due to sample losses in single-cell or small cell ensemble analysis remain with standard sample manipulation and preparation tools. It is also critical to develop multiplexing capable techniques so a substantial number of individual cells can be analyzed simultaneously.

Microfluidics can be advantageous tools to improve sample preparation for protein analysis. Microfluidic techniques involve the isolation and processing of single-cells in the miniaturized environment, and the capability of multiplexing the system to assess small cell ensembles or a large number of individual cells.[11] Microfluidic droplets or valve-controlled wells represent the most common system for single-cell isolation.[12] Microfluidic platforms are often coupled with manipulation techniques, such as optical[13] or magnetic tweezers[14], surface acoustic waves[15], and dielectrophoresis[16–18]. Microfluidic platforms have also been coupled with a wealth of analytical methods yielding novel and functional approaches for single-cell proteomics, such as droplet barcoding,[19] fluorescence immunoassays, electrophoresis and mass spectrometry.[11] Microfluidic barcoding and DNA sequencing represent a powerful approach for protein profiling at the

single cell level.[11,20,19] The single-cell barcode chip (SCBC) is a representative device for a single-cell fluorescence immunoassay.[21,22] Although fluorescence-based methods can be suitable for clinical and point-of care situations, they reach limitations due to spectral overlap of fluorophores for multiplexing. Shubert at al. developed a method for ultrasensitive and automated quantification phenotype responses with single cell resolution using single molecule array (SiMoA) technology. In their work, they demonstrated the absolute quantification of prostate-specific antigen (PSA) expressed in single cancer cells.[23] SiMoA relies on antibody-coated beads to capture single protein molecules and a nano-liter well platform to isolate single beads for signal amplification and fluorescence detection.[24,23]

As the workhorse of proteomics, MS methods have also been explored in combination with microfluidics.[25,26,11,8] Droplet-based microfluidic platforms (water-in-oil systems) can be challenging, because the alternating water and oil plugs can contribute to unstable plumes in electrospray ionization mass spectrometry (ESI-MS).[11] To avoid the oil, nano-liter air-water droplets have been used with LC-MS/MS, involving a complex multistep sample preparation.[27] Open face nano-wells or surface areas with different properties allow the use of droplet-based approaches without oil, which have also been combined with LC-MS.[26] Another approach reaching single cell sensitivity is cell isolation and sample preparation on-chip coupled with LC-MS or LC-MS/MS.[25,26,28,29]

Interfaces with MALDI-TOF-MS (MALDI-MS in short) allow the integration of microfluidic sample processing without fluidic connections to the MS system.[30] In addition, MALDI-MS compared to other MS techniques allows for higher tolerance to salts and detergents as well as the production of single charged ions, which minimizes the complexity of the spectra. However, only a few approaches for single-cell analysis have been reported using MALDI-MS,[31,32,30] and even fewer have integrated microfluidics.[33–36,32]

Previously, we reported the ongoing development of the integrated microfluidic assay in tandem with MALDI mass spectrometry (MIMAS) for protein detection in small cell ensembles.[37,38] The MIMAS platform has been used to detect Bcl-2 protein from cell-free media[38] and from MCF-7 breast cancer cells suspension.[37] Bcl-2 is a key protein in cell apoptosis, and thus of relevance in biological and clinical studies. In our latest work, we successfully incorporated cell lysis in the MIMAS workflow, demonstrating protein release during cell lysis within nanoliter scale wells on the microfluidic platform [37] and further Bcl-2 protein immunocapture and detection from the cell lysate on-chip. The antibodies were first immobilized on-chip prior to cell lysis, and then exposed to subsequent cell lysis freezing and thawing cycles, which adversely affected their binding reactivity. Moreover, quantification of Bcl-2 protein released from the lysed MCF-7 cells was not achieved.

Here, we explored an alternative workflow including different immobilization and binding steps to avoid losses in the antibody reactivity and improve the protein immunocapture in the MIMAS device. The workflow resulted in the successful quantification of Bcl-2 protein from 26 to 223 MCF-7 cells in 8.75 nL wells. An additional innovation is the introduction of smaller volume wells (4 nL), also demonstrating Blc-2 quantification within 8 to 19

cells. We expect the MIMAS approach optimization described in this work to allow the quantitative assessment of other relevant proteins in small cell ensembles. Furthermore, a combination of design update, improvement on the antibody immobilization technique and use of a higher sensitivity instrumentation are considered to enhance the MIMAS approach for the assessment of targeted protein quantification in single cells.

METHODS

Materials

MCF-7 cells, eagle's minimum essential medium (EMEM), fetal bovine serum (FBS), Trypsin, and Dulbecco's phosphate-buffered saline (DPBS) were obtained from ATCC (USA). Acetonitrile, acetone, isopropanol, ethanol, alpha-cyano-4-hydroxycinnamic acid (α-CHCA), human Bcl-2 protein, anti-Bcl-2 antibody, bovine serum albumin (BSA), and bovine insulin were purchased from Sigma-Aldrich (USA). Synthetic peptide FATVVEELFR (m/z 1210.6) and isotope labeled peptide FATVVEEL(13C15N)FR (m/z 1217.6) were purchased from GenScript USA Inc. Polydimethylsiloxane (PDMS) was purchased from Dow Corning Corporation (USA). Indium tin oxide (ITO) coated glass slides (100 ohm/sq) were obtained from NANOCS (USA). Tridecafluoro-1, 1, 2, 2-tetra-trichlorosilane (TTTS) was purchased from Gelest (USA). Isopropanol and acetone were from VWR (USA). SU-8 2075 photoresist and SU-8 developer were from MicroChem (USA). Trypsin for protein digestion on the MIMAS platform was purchased from Promega (USA).

Microfluidic Platform Fabrication and Assembly

The double-layer MIMAS devices were designed and fabricated as previously reported. [37,38] Briefly, the microfluidic platform consists of five consecutive pairs of wells separated by normally-closed valves (Fig. 1a) formed by two polydimethylsiloxane (PDMS) layers, a control and a fluidic layer. The templates were fabricated by photolithography using SU-8 2075 resulting in approximately 25 and 40 μm structure height in the fluidic and control layer, respectively. The fluidic layer was fabricated by spin coating the PDMS (15:1 base to curing agent) over the template for 30 s and curing at 65°C for 35 min. A calibration curve to determine the thickness of the resulting PDMS layer after spin coating was obtained by testing different velocities (all for 30 s and 300 rpm/s acceleration), curing the PDMS and measuring the PDMS layer thickness with a profilometer after removing a portion of PDMS at different positions on the template (see Figure S-1). Based on the calibration curve, a ~56 μm PDMS layer was used to create a 31 μm valve membrane over the channels with 25 μm height. The control layer was fabricated by pouring the PDMS (10:1 base to curing agent) over the template, degassing the PDMS and curing at 65 °C for 35 min. The control layer was peeled-off from the template and the devices were cut and aligned over the fluidic layer using a stereomicroscope. Next, the two layers together were cured at 65°C overnight, then peeled off from the template and reservoirs were punched. The PDMS manifold was treated with oxygen plasma for 90 s at medium FR setting and then incubated at 80°C for 30 min before assembling it with a clean indium tin oxide (ITO) coated glass slide. The valve function was confirmed by applying vacuum to the pneumatic reservoirs and the resulting deflection was verified by microscope inspection. After performing the assay

as stated below, the PDMS manifold was discarded, and the ITO-covered glass slide was washed with acetone, isopropanol and water twice. Prior to reuse, the presence of the ITO layer was confirmed by conductivity measurement.

Cell Culture

MCF-7 human breast cancer cells were cultured in EMEM mixed with L-glutamine, 10% fetal bovine serum and 0.01 mg/mL bovine insulin at 37 °C. The cells were passaged every five days. The EMEM medium in the flask was removed by vacuum using a pipette tip attached to a hose and a vacuum pump and washed by 7 mL DPBS. The DPBS buffer was then removed by vacuum. Then, 2 mL of cell stripper solution was added followed by an incubation at 37 °C for 10 min to strip the cells from the flask surface. Three mL fresh cell culture medium was then added and the cell solution in the flask was transferred to a tube and centrifuged at 4°C for 3 min. Cells were counted in microfluidic wells using a microscope (IX71, Olympus, USA).

Bcl-2 Analysis in the MIMAS Device

Protein solutions of the FATVVEELFR peptide (m/z 1210.6) were prepared at different concentrations (in cell-free medium), mixed with the matrix solution (saturated solution of α-CHCA in 40% acetonitrile and 0.1% trifluoroacetic acid), and loaded into the MIMAS device (n=5) for MALDI-MS analysis to obtain the limit of detection (LOD). This peptide corresponds to the peptide used for quantification in the cell assay (see Mass Spectrometry Analysis section for details in the analysis and LOD determination). Schematics of the MIMAS device are provided in Figure 1a.

In addition, the sensitivity of the immunocapture assay in the MIMAS device was investigated with Bcl-2 solutions at various concentrations and the entire workflow (except for the cell lysis) was performed as shown in Figure 1b (steps 2–6). Anti-Bcl-2 (0.05 mg/mL) was immobilized on fluidic line II (containing wells II) in a humidity chamber for 2 h. Wells were then washed three times with 20 mM sodium phosphate buffer. Next, BSA (1% in phosphate buffer) was incubated in fluidic line II for 30 min to prevent nonspecific adsorption, and then washed three times with phosphate buffer. Bcl-2 protein solution was added to fluidic line I and valve line C was opened to mix the content between wells I and II. Then, the device was incubated for 1 h at room temperature (RT) for immunocapture. Both fluidic lines were washed three times with 50 mM NH_4HCO_3 buffer afterwards. Trypsin (0.1 μg/μL) was added to fluidic line II and incubated for 12 h at 36°C in a humidity chamber. Matrix solution (saturated solution of α-CHCA in 40% acetonitrile and 0.1% trifluoroacetic acid) and isotope-labeled peptide (1217.6 m/z) were added to wells I and mixed with the digested Bcl-2 in wells II by opening valve line C. Once dried, the PDMS manifold was removed to allow MALDI MS analysis with a Bruker Microflex instrument (Bruker, Germany) directly from the ITO target.

Digestion Efficiency at Various Bcl-2 Concentrations

The digestion efficiency was studied in solution and on-chip within a range of initial Bcl-2 protein concentrations. Bcl-2 protein solutions were prepared using 50 mM ammonium bicarbonate to the desired concentration. Trypsin solution was prepared at a concentration

of 0.1 μg/μL using 50 mM ammonium bicarbonate. In an Eppendorf tube, 10 μL of the Bcl-2 solution and 2 μL of the trypsin solution were mixed and incubated for 12 h at 36 °C. After the digestion, 1.5 μL of the isotope labeled peptide (m/z 1217.6) were added to the mixture (at a concentration equivalent to the Bcl-2 initial moles in solution), followed by 5 μL of the matrix solution (saturated solution of α-CHCA in 40% acetonitrile and 0.1% trifluoroacetic acid). The solution was mixed and then spotted on an ITO coated glass slide surface and dried at room temperature. Once dried, the sample was analyzed by MALDI-MS using reflectron mode. The resulting peaks of the tryptic peptide (m/z 1210.6) and standard (m/z 1217.6) were compared to determine the digestion efficiency (tryptic peptide/standard). Similarly, on-chip digestion was performed by pre-mixing 10 μL of the Bcl-2 solution and 2 μL of the trypsin solution followed by loading the mixture on the MIMAS device using fluidic line I. The device was incubated for 12 h at 36 °C in a humidity chamber. Then, 5 μL of the matrix solution and 1.5 μL of the isotope labeled peptide (at a concentration equivalent to the Bcl-2 moles on-chip) were pre-mixed and loaded into the device using fluidic line II. The center valve was actuated to mix the content of the fluidic lines I and II. The device was then left at RT for at least 4 h for the solutions to co-crystallized. Lastly, the PDMS manifold was removed and the crystals were analyzed by MALDI-MS using reflectron mode.

Bcl-2 Quantification from MCF-7 Cells in the MIMAS Device

The MIMAS assay workflow for the MCF-7 loading and lysis on-chip and the immunocapture on-chip of Bcl-2 protein is shown in Figure 1b. First, a 1% bovine serum albumin (BSA) solution was loaded into the fluidic line I and incubated for 1 h to avoid surface adsorption and non-specific binding. Then, the fluidic line I was washed with phosphate buffer followed by the loading of MCF-7 cell suspension. Cells on each well were counted using a microscope (see a representative image in Figure S-2). Cells were lysed through 8 cycles of freezing at −20°C and then thawing at 36°C, as previously reported.[37] Anti-Bcl-2 (0.05 mg/mL) was immobilized on fluidic line II in a humidity chamber for 2 h. Subsequently, wells were washed with 20 mM sodium phosphate buffer followed by an additional BSA (1%) blocking step, and a buffer wash. Valve line C was actuated (opened and closed multiple times during 2 min) to mix the content between wells I and II. With all valves closed, immunocapture of Bcl-2 was carried out by incubating the device for 1 h at RT, followed by washing of both fluidic lines with 50 mM NH_4HCO_3 buffer. Trypsin (0.1 μg/μL) was added to the channel II and incubated for 12 h in a humidity chamber at 36°C. Matrix solution (saturated α-CHCA in 40% acetonitrile and 0.1% trifluoroacetic acid) and isotope-labeled peptide (1217.6 m/z) were added to wells I and mixed with the digested Bcl-2 in wells II by actuating valve line C. The device was set aside at room temperature for co-crystallization for at least 4 h. Once dried, the PDMS manifold was removed to expose the analyte-matrix crystals on the substrate surface used as target in the MS instrument.

To investigate optimal antibody immobilization parameters, incubation time and temperature were varied using two methods (I and II). In method I, incubation steps were carried out at 36°C while in method II incubation steps were at 4°C, both in a humidifying chamber. In method I, antibody immobilization was carried out for 0.5, 1 and 2 h. Similarly, for method II, antibody immobilization was tested for 1 and 2 h. For both methods, the center valve

line C was opened after the antibody incubation and washing to mix the cell lysate with the content of wells II. Immunocapture of Bcl-2 protein from the cell lysate was accomplished by incubation at RT for 1 h. After thorough washing steps, trypsin was added to fluidic line II and the devices were incubated at 36°C during 12 h for digestion. Matrix solution was loaded into fluidic line I and valve line C was opened to mix the content in fluidic line I and II. Once the sample-matrix mixture was co-crystallized, the PDMS manifold was removed. The MS analysis was performed on the remaining co-crystals by depleting the entire material of each well.

Mass Spectrometry Analysis

MS analysis was performed in reflector mode for all analyses. Laser movement was controlled manually, and between 1500 to 2500 laser (or until sample depletion) shots were used to acquire spectra. An external calibration was performed for each analysis by spotting insulin with the matrix solution on the target slide surface. Baseline subtraction and peak identification were performed on the resulting spectra using flexAnalysis (Bruker, Germany). Bcl-2 fragments were identified by MASCOT search.[38] The resulting data was analyzed with Origin, version 9.4, (OriginLab Corporation, USA). The peak area of the peptides was estimated using the peak analysis function in Origin, accounting for the peptide peak with all corresponding isotopic peaks.[39–41] The limit of detection (LOD) was determined based on the linear fitting of the calibration curve obtained as $3.3*\sigma/S$, where σ represents the standard deviation of the y-intercept (or blank) and S represents the slope. The number of Bcl-2 molecules was estimated by comparing the peak areas of the tryptic peptide 1210.6 m/z and the isotope labeled peptide 1217.6 m/z, corrected by the digestion efficiency.

RESULTS AND DISCUSSION

Bcl-2 Protein Analysis in MIMAS Device

In this study, we targeted Bcl-2 protein, a key protein relevant in cell apoptosis, from MCF-7 breast cancer cells. Seven peptide peaks were identified as Bcl-2 tryptic peptides from digestion in our previous work (m/z $[M+H]^+$ 1052.0, m/z $[M+H]^+$ 1210.6, m/z $[M+H]^+$ 1950.8, m/z $[M+H]^+$ 1994.8, m/z $[M+H]^+$ 2295.1, m/z $[M+H]^+$ 2886.6, and m/z $[M+H]^+$ 3596.8) using an on-chip workflow.[37,38] Here, an alternative workflow was developed as outlined in the methods section to improve the antibody binding step and allow for on-chip cell lysis with subsequent protein quantification. The Bcl-2 tryptic peptide with m/z 1210.6 (FATVVEELFR) was chosen for quantification as it resulted in the highest S/N ratio when performing trypsin digestion of Bcl-2 in solution from cell lysate. Correspondingly, the isotope-labeled peptide FATVVEEL(13C,15N)FR (m/z 1217.6) was used as an internal standard to compare to the selected tryptic peptide for quantification. We assessed the sensitivity of the MIMAS platform for the FATVVEELFR tryptic peptide as well as the protein Bcl-2 subjected to the immunoassay and enzymatic digestion in the MIMAS device and explored to quantitatively assess Bcl-2 from small cell ensembles in the MIMAS platform.

First, the limit of detection (LOD) of the Bcl-2 tryptic peptide FATVVEELFR (m/z 1210.6) was assessed in the MIMAS device using an equivalent non-labelled synthetic peptide. Considering the range of high abundance proteins in single cells to be between 10^5 and 10^6 copies of a particular protein, concentrations between 1.4 and 280 nM were used for the standard curve based on the 8.75 nL well volume of the established MIMAS platform. Figure 2 shows the obtained standard curve. A weighted linear regression was used to obtain the LOD, which was determined as 11.22 nM, equivalent to 5.91×10^7 Bcl-2 peptide molecules per well.

Subsequently, the assay workflow depicted in Figure 1b was performed in the MIMAS device using Bcl-2 protein. Freezing and thawing cycles were not performed in this case, as cell lysis was not necessary (step 1 in Figure 1b was omitted). Antibody immobilization and non-specific site blocking with BSA were performed in fluidic line II prior to loading of Bcl-2 protein in fluidic line I. This is the line where the cell lysate is loaded when the assay is performed with cells. The content of both wells was mixed through actuating valve line C to expose the protein to the antibodies and induce the immunocapture step in line II. Then, washing of wells, trypsin digestion and the addition of matrix with isotope-labeled peptide as internal standard were performed. The Bcl-2 protein concentration was varied while maintaining the internal standard at 1.4 μM or at 140 nM. The resulting tryptic peptide with m/z 1210.6 was used and compared to the internal standard peptide m/z 1217.6 for quantification. Figure 2b shows the ratio of the Bcl-2 tryptic peptide FATVVEELFR (m/z 1210.6) and the internal standard FATVVEEL(13C,15N)FR (m/z 1217.6) based on the calculated peak area, which will subsequently be used to determine the number of Bcl-2 molecules detected. A weighted linear regression shows the linearity of the Bcl-2 tryptic peptide and internal standard relationship in the concentration range employed.

Digestion Efficiency at Various Bcl-2 Concentrations

The digestion efficiency plays an important role for the number of molecules quantified from cells with the presented workflow. To determine the effect of the initial Bcl-2 protein concentration on the digestion efficiency, we performed the trypsin digestion at different concentrations of Bcl-2 and a fixed trypsin concentration. The experiments were performed in Eppendorf tubes (in-solution) and on MIMAS devices (on-chip). By using the internal standard FATVVEEL(13C,15N)FR corresponding to the heavy counterpart of the Bcl-2 tryptic peptide FATVVEELFR at the same concentration as the initial Bcl-2 concentration for each condition, we estimated the digestion efficiency as the ratio of the Bcl-2 tryptic peptide peak area and the internal standard peak area. Figure 3 shows the in-solution and on-chip digestion efficiency for a range of different Bcl-2 protein concentrations performed. Three important aspects can be deducted from Figure 3. First, the digestion efficiency decreases with decreasing Bcl-2 concentration from about 90% at the highest concentrations to about 40% at the lowest. This signifies that the digestion efficiency needs to be corrected for low Bcl-2 concentrations, when assessing small cell ensembles in the MIMAS device. Second, in-solution and on-chip digestion efficiencies are the same. The third observation is that the digestion efficiency does not seem to decrease below 700 nM. Therefore, we use a digestion efficiency of 40% in the reminder of this manuscript for quantitative assessment.

The reason for a reduced digestion efficiency can have several origins and may be related to the analyte and enzyme concentrations, the volume, the environment, and digestion time. In our previous work, we determined an optimum time for digestion of 12 h (in-solution and on-chip) which we adopted in this work.[37] Studies by others comparing trypsin digestion in-solution and on-chip (in microfluidic chambers or wells) have observed a larger on-chip efficiency caused by the reduction of diffusion distances leading to an increased number of encounters between the protein (substrate) and enzymes.[42–44] However, in our MIMAS approach, the protein molecules are captured by the antibodies immobilized on the MIMAS well surface, which is different from free molecules being digested in solution. Seok et al. [45] reported a detailed study on the variation of the digestion efficiency based on the ratio of trypsin to affinity-captured protein, digestion time, composition of the reaction buffer, and protein concentration. They observed no changes in the digestion efficiency based on the initial amount of protein available when the digestion is performed on-chip compared to a dependency of the digestion efficiency on the protein concentration when performed in-solution. This study supports our findings and reasoning for considering a constant 40% digestion efficiency for protein quantification.

Bcl-2 Quantification from MCF-7 Cells in the MIMAS Device

To detect and quantify Bcl-2 protein originating from MCF-7 cells, the MIMAS assay was performed as shown in Figure 1b. We previously reported a workflow with the current MIMAS platform design, where we successfully detected spiked Bcl-2 protein from cell lysate. [37] However, a quantitative assessment of Bcl-2 protein released from cells lysed on-chip was not achieved. We considered the exposure of the antibodies during the freezing and thawing cycles as the main cause for not reaching the required sensitivity for a quantitative assessment. Consequently, in this work we present a different assay workflow. Previously, antibodies were immobilized in fluidic line I before the cell lysis. Here, we first loaded the cell suspension to fluidic channel I and performed the cell lysis on-chip through eight freezing and thawing cycles. A surface coating treatment with BSA was performed before the cell loading to avoid surface adsorption of the cell lysate. After cell lysis, the antibodies were loaded to fluidic line II to perform the immobilization and blocking steps. Next, we actuated valve line C to mix the content of fluidic I and II and induce the immunocapture in fluidic line II (where antibodies were immobilized). Mixing of the well contents was achieved by actuating the valve in between them for 2 min, as previously determined to achieve sufficient mixing.[38] The purpose of this new workflow was to improve the assay sensitivity by increasing the number of active immobilized antibodies.

Furthermore, to determine the optimal parameters for the antibody immobilization, incubation time and temperature were varied as shown in Figure 4a. The non-specific site blocking step was kept constant for both methods, but it was reduced to 30 min compared to our previous work where it was carried out for 1 h. [37] As the cell lysate is already in well I during the antibody immobilization and blocking steps, protein adsorption to the surface and degradation were a concern. In an aim to reduce the overall time of the cell lysate remains in the well, we reduced the BSA incubation time and tested different antibody immobilization temperatures and times. Non-specific binding was effectively prevented through a 30 min BSA incubation both at 36°C and at 4°C, as demonstrated in the control experiment without

the binding antibody shown in Figure 4b and 4d. Both temperature conditions lacked peaks identified as Bcl-2 tryptic peptides, however, several peaks from trypsin auto-digestion were apparent. In contrast, when an antibody immobilization step was carried out followed by a blocking step, Bcl-2 tryptic peptides were detected after the trypsin digestion step and matrix deposition on chip. Figure 4c and 4e show representative mass spectra for the two temperature conditions with the antibody immobilization carried out for 2 h. An inset focused on the m/z 1210 Bcl-2 tryptic peptide and internal standard is also presented in both figures.

The number of Bcl-2 tryptic peptides identified in each well varied between two and six depending on the temperature and duration of the antibody immobilization step (see Figure S-3). For method I (36°C), the antibody immobilization was carried out for 0.5, 1 and 2 h. When the antibody immobilization was carried out for 0.5 and 1 h, the Bcl-2 tryptic peptide m/z 1210.6 was rarely observed but other Bcl-2 tryptic peptides were observed. Antibody immobilization during 1 h using method II (4°C) lacked Bcl-2 tryptic peptides in most of the wells. For both methods, the 2 h antibody immobilization showed the highest number of Bcl-2 tryptic peptides found compared to the same method with shorter times.

Subsequently, we investigated the amount of Bcl-2 detected in the MIMAS wells for the entire assay with integrated cell lysis. The concentration used of the isotope labeled internal standard peptide was 140 nM, which is equivalent to 7.38×10^8 molecules. By determining the peak area ratio of FATVVEELFR and FATVVEEL(13C,15N)FR, we determined the number of Bcl-2 molecules in each well, considering a digestion efficiency of 40%. The number of Bcl-2 molecules per well ranged from 3.92×10^8 molecules to 17.40×10^8 molecules. For all wells, we assessed the number of cells per well prior to the lysis step, thus, the quantified Bcl-2 amount can be compared with the number of cells per well, which varied from 26 to 223 cells. Figure 5a shows the number of molecules detected per well compared to the number of MCF-7 cells in each corresponding well. With this information, the average number of Bcl-2 molecules per cell was also obtained and reported in Figure 5b. It is interesting to note that the highest amount was found for the least cells counted per well. Normalized by the number of cells per each well, Figure 5b demonstrates that the Bcl-2 amount was in range of 4×10^6 to 62×10^6 molecules per cell, which is an expected range for a high abundant protein in a single cell. Also of note is that the highest amount of Bcl-2 was detected for the least amount of cells per well. Wells containing less than 30 cells resulted in an average number of molecules per cell from 5.2×10^7 to 6.2×10^7. Differences in the number of Bcl-2 protein molecules from cells is expected due to cell heterogeneity, where the number of Bcl-2 molecules varies from cell to cell. As Bcl-2 is involved in the apoptosis of cells, the number of Bcl-2 molecules may vary substantially based on the stress each cell was exposed to during the cell lysis and handling procedure. [46]

However, the phenomenon observed in Figure 5 may be caused by multiple effects besides cell heterogeneity, such as MS ion suppression and masking effects caused by the cell lysate. The smaller Bcl-2 amount in wells with > 30 cells can be attributed to masking effects due to the biomolecular complexity of the cell lysate. This effect may be aggravated with larger cell numbers per well, as previously observed [37,47], reducing detection capabilities for the low molecular weight peptides used for quantification.[48,49] In our previous work,

a masking effect was reported when using spiked cell lysate, with 14 nM and 140 nM Bcl-2 protein.[37] Accordingly, an approximate of 30 cells in an 8.75 nL well is equivalent to 3,400 cells/μL, a range where the 1210.6 m/z peptide signal is reduced by > 90% compared to a cell count of 5 cells/μL. A single cell per well is equivalent to 114 cell/μL, where these effects have been demonstrated to be greatly reduced. [37] In addition, ion suppression effects have been reported to show an intensity reduction of target analytes at high concentrations when working with complex matrices.[50] The digestion efficiency can also play a significant role influencing this effect. As observed in Figure 3, the digestion efficiency varies based on the initial Bcl-2 concentration. Based on this finding, we have adjusted the calculation of the number of proteins apparent in MCF-7 cells with a digestion efficiency of 40% consistent with the observations at low concentrations as observed with the cells (between 74.4 nM and 300 nM). Finally, we remark that the MIMAS assay will reach limitations through the amount of active antibody available for immunocapture, which needs to be assessed quantitatively in further studies.

Next, we turn to a comparison of the MIMAS device for protein quantification with other approaches in the literature, the SCBC [22,21] and SiMoA [23] technologies, which can reach single cell protein sensitivity. The SCBC technology consists of the isolation of a defined number of cells in a 2 nL microchamber with an antibody array for the capture and detection of targeted proteins, with cell lysis performed on-chip. On the other side, SiMoA technology is a quantitative protein analysis method based on antibody-coated beads isolated in a microarray, based on an enzyme conjugate for sensitive fluorescence detection. Both technologies are fluorescence-based approaches, which can be limited by fluorophore availability, interactions with the analyte of interest, and spectral overlap of fluorophores. In this regard, our work avoids the use of fluorescent tags or microscope imaging for detection. We take advantage of the high sensitivity and specificity of mass spectrometry, which besides allowing for the detection and quantification of proteins can allow for PTM or isoform identification.

We further note that we aim to perform a quantitative assessment of a target protein in the smallest cell count possible towards reaching single cell sensitivity with the MIMAS approach. However, the current capabilities of the MIMAS approach can also be used for applications that do not require single cell sensitivity. For example, our preliminary MIMAS work has been used to assess proteins in blood serum,[51] and quantitatively identify proteins from human tissues.[52] The current technology allows for the detection of physiological levels of proteins from complex matrices such as blood serum, cell lysates and tissue cells.

MIMAS Workflow in 4 nL Wells

The cell lysis on-chip allows confining the cell lysate within a defined volume, avoiding further dilutions or losses during the manipulation of the sample. The well volume can be modified via the well dimensions. Considering the ultimate goal of applying this approach for targeted single-cell protein analysis, we explored the reduction in the well volume. To test a smaller volume, wells with dimensions of 300 × 300 × 25 μm constituting a volume of

4 nL were fabricated and used for the MIMAS assay with MCF-7 cells (see Figure S-4a for an image).

First, we analyzed a series of concentrations of the synthetic peptide equivalent to the Bcl-2 tryptic peptide m/z 1210.6 with the updated design (see Figure S-4b). The LOD based on the weighted linear regression was determined as 14.85 nM, which is equivalent to 3.57×10^7 molecules of Bcl-2 protein. The reduction of approximately 60% in the well volume thus resulted in an increased sensitivity. We consider that this increase in sensitivity is due to the MS ionization process. The matrix solution is mixed with the analyte in excess of solvent to allow the crystallization by solvent evaporation. Then, during MS analysis, the matrix absorbs the laser energy while it is simultaneously volatilized, releasing the analyte in the gas phase as charged ions with minimal fragmentation. Although MALDI-MS is a technique widely used for protein and peptide analysis, the ionization process and ion suppression effects involved are still poorly understood.[53] Similar Bcl-2 peptide concentration mixed with the matrix solution in different volumes may affect the drying and analyte-matrix crystallization process as well as the ionization process during the MS analysis. The sample-matrix preparation can still be an empirical technique,[54] requiring the optimization for specific analytes.[55–57] As the process can vary depending on the analyte, we tested a mixture of different proteins (somatostatin, calcitonin, insulin and cytochrome c) with the same matrix solution in both MIMAS designs (8.75 nL and 4 nL wells). As demonstrated in Table S-1, we also observed an increase in S/N for the four other assessed proteins when quantified from the 4 nL wells as compared to the 8.75 nL. This is in agreement with the sensitivity increase observed for the here presented Bcl-2 study. The improved sensitivity in the 4 nL wells compared to the 8.75 nL wells could result from variations in the MALDI co-crystallization and ionization process.

Furthermore, the workflow described in Figure 1b and method II for the antibody immobilization was used to assess Bcl-2 from MCF-7 cells in the smaller 4 nL well design. An average of 14 (ranging from 8 to 19) cells was present in each well. A representative spectrum of Bcl-2 tryptic peptides is shown in Figure 6a. An average of 2.23×10^8 molecules of Bcl-2 was calculated per 4 nL well (Figure 6b). Based on the obtained number of molecules per well and the corresponding cell count in each well, an average of 19.34×10^6 Bcl-2 molecules resulted per cell (Figure 6c). For wells with 8.75 nL volume ($500 \times 500 \times 25$ μm), the number of cells per well varied between 26 and 223, with an average of 89 ± 50 cells per well. Although the average number of cells in the 4 nL wells is $^1/_6$ of the average number sampled in the 8.75 nL wells, the MIMAS workflow in the smaller wells also allow to assess a similar number of Bcl-2 molecules per cell. The number of Bcl-2 molecules detected per well in the 8.75 nL wells is significantly different from the number of molecules detected in the 4 nL wells, however, there is no significant differences between the number of Bcl-2 molecules per cell. Carrying out the entire assay in both well volumes provides Bcl-2 amounts from small cell ensembles in excellent agreement.

Finally, we discuss further downscaling of the well size in the MIMAS device for reducing the number of cells assessed with the ultimate goal of single cell analysis. Several key factors will contribute to a future downscaling and optimization. Currently, we are using randomly oriented antibodies immobilized on the ITO surface coated glass slide.[58]

The orientation of antibodies has a critical impact in the antibody reactivity and binding capacity.[59–61] Thus, the immunocapture in the MIMAS device can be improved by implementing different immobilization techniques to increase the amount and orientation of active antibodies, such as including the PDMS surface in the immobilization strategy by suitable activation approaches[62] or providing surface functional groups for antibody immobilization.[63–65] On the other hand, the observed lysate masking effect could be further reduced through even smaller well size and fewer captured cells. Additionally, MALDI-MS technology is continuously improving, increasing its sensitivity and resolution capabilities and allowing detection of low abundance analytes from complex sample matrices.[66,67] Although we observed as increase in sensitivity based on the well size decrease for Bcl-2 peptide and other proteins as shown in Table S-1, there is a physical limitation on how small the well design can be reduced while maintaining all workflow steps required for the entire assay. Guaranteeing ease of fabrication, handling of human cells comparable to MCF-7 cells as well as aspect ratios allowing proper valve actuation we define the well size to amount in 100 μm x 100 μm x 25 μm. In this case, the well volume would be ~63 pL, for which we estimate about 3×10^6 active antibody molecules immobilized in the surface considering about 5% of the immobilized antibodies are active. Thus, such a well size would be suitable to detect proteins from single cells in copy numbers of ~ 10^6. We hypothesize that a combination of well size reduction, antibody immobilization optimization and decrease of the number of cells could improve the sensitivity of the MIMAS assay, which together with the newest state-of-the-art MALDI-MS instruments, can ultimately allow the analysis of targeted proteins from single cells.

CONCLUSION

An integrated microfluidic platform for sample preparation in tandem with MALDI-MS has been developed and optimized for the analysis of targeted proteins from small cell ensembles. The on-chip sample preparation steps involve cell lysis, immunocapture of the target protein, tryptic digestion and co-crystallization with matrix solution for the MALDI-MS analysis are carried out in parallel for five assays. We have successfully quantified Bcl-2 protein extracted from MCF-7 cells on-chip using an isotope labeled peptide as internal standard for the quantification. With this work, we demonstrate that the MIMAS approach is suitable for the detection and quantification of proteins from cell ensembles in combination with MALDI-MS. We have also explored a reduction of the well size, where quantifiable amounts of Bcl-2 from small cell ensembles down to ~10 cell were detected. Future work will focus on further optimization of the protein-capturing efficiency and sensitivity increase towards single cell protein analysis. The MIMAS approach is a promising tool we anticipate soon to be used for the identification and quantification of relevant targeted proteins from small cell ensembles down to single cells, with the ability for multiplexing through microfluidic parallelization and automation.

Supplementary Material

Refer to Web version on PubMed Central for supplementary material.

ACKNOWLEDGEMENTS

Research reported in this publication was supported by National Institute on Aging of the National Institute of Health under Award Number R21AG067488. We also thank, Dr. Mouneimne (UofA Cancer Center) for sharing MCF-7 cells and acknowledge the ASU MS Core Facility for the mass spectrometry use. BioRender was used for the creation of several figures in this manuscript. JCV acknowledges the partial financial support by CONACYT through a doctoral fellowship.

REFERENCES

1. Altschuler SJ, Wu LF (2010) Cellular Heterogeneity: Do Differences Make a Difference? Cell 141 (4):559–563. 10.1016/j.cell.2010.04.033 [PubMed: 20478246]
2. Cheung TK, Lee C-Y, Bayer FP, McCoy A, Kuster B, Rose CM (2021) Defining the carrier proteome limit for single-cell proteomics. Nat Methods 18 (1):76–83. 10.1038/s41592-020-01002-5 [PubMed: 33288958]
3. Liu J, He H, Xie D, Wen Y, Liu Z (2021) Probing low-copy-number proteins in single living cells using single-cell plasmonic immunosandwich assays. Nat Protoc 16 (7):3522–3546. 10.1038/s41596-021-00547-9 [PubMed: 34089021]
4. Qian M, Yan F, Yuan T, Yang B, He Q, Zhu H (2020) Targeting post-translational modification of transcription factors as cancer therapy. Drug Discov Today 25 (8):1502–1512. 10.1016/j.drudis.2020.06.005 [PubMed: 32540433]
5. Chatterjee B, Thakur SS (2018) Investigation of post-translational modifications in type 2 diabetes. Clin Proteom 15 (1):32. doi:10.1186/s12014-018-9208-y
6. Nakamura T, Lipton SA (2016) Protein S-Nitrosylation as a Therapeutic Target for Neurodegenerative Diseases. Trends in pharmacological sciences 37 (1):73–84. 10.1016/j.tips.2015.10.002 [PubMed: 26707925]
7. Ghaemmaghami S, Huh W-K, Bower K, Howson RW, Belle A, Dephoure N, O'Shea EK, Weissman JS (2003) Global analysis of protein expression in yeast. Nature 425 (6959):737–741. 10.1038/nature02046 [PubMed: 14562106]
8. Slavov N (2021) Single-cell protein analysis by mass spectrometry. Curr Opin Chem Biol 60:1–9. 10.1016/j.cbpa.2020.04.018 [PubMed: 32599342]
9. Kelly RT (2020) Single-cell Proteomics: Progress and Prospects. Mol Cell Proteomics 19 (11):1739–1748. 10.1074/mcp.R120.002234 [PubMed: 32847821]
10. Belov ME, Gorshkov MV, Udseth HR, Anderson GA, Smith RD (2000) Zeptomole-sensitivity electrospray ionization--Fourier transform ion cyclotron resonance mass spectrometry of proteins. Anal Chem 72 (10):2271–2279. 10.1021/ac991360b [PubMed: 10845374]
11. Liu Y, Chen X, Zhang Y, Liu J (2019) Advancing single-cell proteomics and metabolomics with microfluidic technologies. Analyst 144 (3):846–858. 10.1039/C8AN01503A [PubMed: 30351310]
12. Prakadan SM, Shalek AK, Weitz DA (2017) Scaling by shrinking: empowering single-cell 'omics' with microfluidic devices. Nat Rev Genet 18 (6):345–361. 10.1038/nrg.2017.15 [PubMed: 28392571]
13. Shah GJ, Ohta AT, Chiou EPY, Wu MC, Kim C-JC (2009) EWOD-driven droplet microfluidic device integrated with optoelectronic tweezers as an automated platform for cellular isolation and analysis. Lab Chip 9 (12):1732–1739. 10.1039/B821508A [PubMed: 19495457]
14. Ali-Cherif A, Begolo S, Descroix S, Viovy J-L, Malaquin L (2012) Programmable Magnetic Tweezers and Droplet Microfluidic Device for High-Throughput Nanoliter Multi-Step Assays. Angew Chem Int Edit 51 (43):10765–10769. 10.1002/anie.201203862
15. Collins DJ, Morahan B, Garcia-Bustos J, Doerig C, Plebanski M, Neild A (2015) Two-dimensional single-cell patterning with one cell per well driven by surface acoustic waves. Nat Commun 6:8686. 10.1038/ncomms9686 [PubMed: 26522429]
16. Hunt TP, Issadore D, Westervelt RM (2008) Integrated circuit/microfluidic chip to programmably trap and move cells and droplets with dielectrophoresis. Lab Chip 8 (1):81–87. 10.1039/B710928H [PubMed: 18094765]

17. Kim D, Sonker M, Ros A (2019) Dielectrophoresis: From Molecular to Micrometer-Scale Analytes. Anal Chem 91 (1):277–295. 10.1021/acs.analchem.8b05454 [PubMed: 30482013]
18. Bhattacharya S, Chao T-C, Ariyasinghe N, Ruiz Y, Lake D, Ros R, Ros A (2014) Selective trapping of single mammalian breast cancer cells by insulator-based dielectrophoresis. Anal Bioanal Chem 406 (7):1855–1865. 10.1007/s00216-013-7598-2 [PubMed: 24408303]
19. Shahi P, Kim SC, Haliburton JR, Gartner ZJ, Abate AR (2017) Abseq: Ultrahigh-throughput single cell protein profiling with droplet microfluidic barcoding. Sci Rep 7:44447–44447. 10.1038/srep44447 [PubMed: 28290550]
20. Stoeckius M, Hafemeister C, Stephenson W, Houck-Loomis B, Chattopadhyay PK, Swerdlow H, Satija R, Smibert P (2017) Simultaneous epitope and transcriptome measurement in single cells. Nat Methods 14 (9):865–868. 10.1038/nmeth.4380 [PubMed: 28759029]
21. Ma C, Fan R, Ahmad H, Shi Q, Comin-Anduix B, Chodon T, Koya RC, Liu C-C, Kwong GA, Radu CG, Ribas A, Heath JR (2011) A clinical microchip for evaluation of single immune cells reveals high functional heterogeneity in phenotypically similar T cells. Nature Med 17 (6):738–743. 10.1038/nm.2375 [PubMed: 21602800]
22. Shi Q, Qin L, Wei W, Geng F, Fan R, Shik Shin Y, Guo D, Hood L, Mischel PS, Heath JR (2012) Single-cell proteomic chip for profiling intracellular signaling pathways in single tumor cells. Proc Natl Acad Sci 109 (2):419–424. 10.1073/pnas.1110865109 [PubMed: 22203961]
23. Schubert SM, Walter SR, Manesse M, Walt DR (2016) Protein Counting in Single Cancer Cells. Anal Chem 88 (5):2952–2957. 10.1021/acs.analchem.6b00146 [PubMed: 26813414]
24. Rissin DM, Fournier DR, Piech T, Kan CW, Campbell TG, Song L, Chang L, Rivnak AJ, Patel PP, Provuncher GK, Ferrell EP, Howes SC, Pink BA, Minnehan KA, Wilson DH, Duffy DC (2011) Simultaneous Detection of Single Molecules and Singulated Ensembles of Molecules Enables Immunoassays with Broad Dynamic Range. Anal Chem 83 (6):2279–2285. 10.1021/ac103161b [PubMed: 21344864]
25. Li S, Plouffe BD, Belov AM, Ray S, Wang X, Murthy SK, Karger BL, Ivanov AR (2015) An Integrated Platform for Isolation, Processing, and Mass Spectrometry-based Proteomic Profiling of Rare Cells in Whole Blood. Mol Cell Proteomics 14 (6):1672–1683. 10.1074/mcp.M114.045724 [PubMed: 25755294]
26. Zhu Y, Piehowski PD, Zhao R, Chen J, Shen Y, Moore RJ, Shukla AK, Petyuk VA, Campbell-Thompson M, Mathews CE, Smith RD, Qian W-J, Kelly RT (2018) Nanodroplet processing platform for deep and quantitative proteome profiling of 10–100 mammalian cells. Nat Commun 9 (1):882. 10.1038/s41467-018-03367-w [PubMed: 29491378]
27. Li Z-Y, Huang M, Wang X-K, Zhu Y, Li J-S, Wong CCL, Fang Q (2018) Nanoliter-Scale Oil-Air-Droplet Chip-Based Single Cell Proteomic Analysis. Anal Chem 90 (8):5430–5438. 10.1021/acs.analchem.8b00661 [PubMed: 29551058]
28. Budnik B, Levy E, Harmange G, Slavov N (2018) SCoPE-MS: mass spectrometry of single mammalian cells quantifies proteome heterogeneity during cell differentiation. Genome Biol 19 (1):161. 10.1186/s13059-018-1547-5 [PubMed: 30343672]
29. Specht H, Emmott E, Petelski AA, Huffman RG, Perlman DH, Serra M, Kharchenko P, Koller A, Slavov N (2021) Single-cell proteomic and transcriptomic analysis of macrophage heterogeneity using SCoPE2. Genome Biol 22 (1):50. 10.1186/s13059-021-02267-5 [PubMed: 33504367]
30. Lee J, Soper SA, Murray KK (2009) Microfluidics with MALDI analysis for proteomics —A review. Analytica Chimica Acta 649 (2):180–190. 10.1016/j.aca.2009.07.037 [PubMed: 19699392]
31. Yin L, Zhang Z, Liu Y, Gao Y, Gu J (2019) Recent advances in single-cell analysis by mass spectrometry. Analyst 144 (3):824–845. 10.1039/C8AN01190G [PubMed: 30334031]
32. Mao S, Li W, Zhang Q, Zhang W, Huang Q, Lin J-M (2018) Cell analysis on chip-mass spectrometry. TrAC Trends in Analytical Chemistry 107:43–59. 10.1016/j.trac.2018.06.019
33. Hatakeyama T, Chen DL, Ismagilov RF (2006) Microgram-Scale Testing of Reaction Conditions in Solution Using Nanoliter Plugs in Microfluidics with Detection by MALDI-MS. J Am Chem Soc 128 (8):2518–2519. 10.1021/ja057720w [PubMed: 16492019]

34. Momotenko D, Qiao L, Cortés-Salazar F, Lesch A, Wittstock G, Girault HH (2012) Electrochemical Push–Pull Scanner with Mass Spectrometry Detection. Anal Chem 84 (15):6630–6637. 10.1021/ac300999v [PubMed: 22789113]
35. Küster SK, Fagerer SR, Verboket PE, Eyer K, Jefimovs K, Zenobi R, Dittrich PS (2013) Interfacing droplet microfluidics with matrix-assisted laser desorption/ionization mass spectrometry: label-free content analysis of single droplets. Anal Chem 85 (3):1285–1289. 10.1021/ac3033189 [PubMed: 23289755]
36. Haidas D, Napiorkowska M, Schmitt S, Dittrich PS (2020) Parallel Sampling of Nanoliter Droplet Arrays for Noninvasive Protein Analysis in Discrete Yeast Cultivations by MALDI-MS. Anal Chem 92 (5):3810–3818. 10.1021/acs.analchem.9b05235 [PubMed: 31990188]
37. Yang M, Cruz Villarreal J, Ariyasinghe N, Kruithoff R, Ros R, Ros A (2021) Quantitative Approach for Protein Analysis in Small Cell Ensembles by an Integrated Microfluidic Chip with MALDI Mass Spectrometry. Anal Chem 93 (15):6053–6061. 10.1021/acs.analchem.0c04112 [PubMed: 33819014]
38. Yang M, Nelson R, Ros A (2016) Toward Analysis of Proteins in Single Cells: A Quantitative Approach Employing Isobaric Tags with MALDI Mass Spectrometry Realized with a Microfluidic Platform. Anal Chem 88 (13):6672–6679. 10.1021/acs.analchem.5b03419 [PubMed: 27257853]
39. Wang H, Alvarez S, Hicks LM (2012) Comprehensive Comparison of iTRAQ and Label-free LC-Based Quantitative Proteomics Approaches Using Two Chlamydomonas reinhardtii Strains of Interest for Biofuels Engineering. Journal of Proteome Research 11 (1):487–501. 10.1021/pr2008225 [PubMed: 22059437]
40. Xie F, Liu T, Qian W-J, Petyuk VA, Smith RD (2011) Liquid Chromatography-Mass Spectrometry-based Quantitative Proteomics. Journal of Biological Chemistry 286 (29):25443–25449. 10.1074/jbc.R110.199703 [PubMed: 21632532]
41. Shadforth IP, Dunkley TPJ, Lilley KS, Bessant C (2005) i-Tracker: For quantitative proteomics using iTRAQ™. BMC Genomics 6 (1):145. 10.1186/1471-2164-6-145 [PubMed: 16242023]
42. Lee J, Soper SA, Murray KK (2009) Development of an efficient on-chip digestion system for protein analysis using MALDI-TOF MS. Analyst 134 (12):2426–2433. doi:10.1039/B916556H [PubMed: 19918612]
43. Mouradian S (2002) Lab-on-a-chip: applications in proteomics. Current Opinion in Chemical Biology 6 (1):51–56. 10.1016/S1367-5931(01)00280-0 [PubMed: 11827823]
44. Slovakova M, Minc N, Bilkova Z, Smadja C, Faigle W, Fütterer C, Taverna M, Viovy J-L (2005) Use of self assembled magnetic beads for on-chip protein digestion. Lab on a Chip 5 (9):935–942. 10.1039/B504861C [PubMed: 16100577]
45. Seok H-J, Hong M-Y, Kim Y-J, Han M-K, Lee D, Lee J-H, Yoo J-S, Kim H-S (2005) Mass spectrometric analysis of affinity-captured proteins on a dendrimer-based immunosensing surface: investigation of on-chip proteolytic digestion. Analytical Biochemistry 337 (2):294–307. 10.1016/j.ab.2004.10.042 [PubMed: 15691510]
46. Czabotar PE, Lessene G, Strasser A, Adams JM (2014) Control of apoptosis by the BCL-2 protein family: implications for physiology and therapy. Nature reviews Molecular cell biology 15 (1):49–63. 10.1038/nrm3722 [PubMed: 24355989]
47. Albalat A, Stalmach A, Bitsika V, Siwy J, Schanstra JP, Petropoulos AD, Vlahou A, Jankowski J, Persson F, Rossing P, Jaskolla TW, Mischak H, Husi H (2013) Improving peptide relative quantification in MALDI-TOF MS for biomarker assessment. Proteomics 13 (20):2967–2975. 10.1002/pmic.201300100 [PubMed: 23943474]
48. Annesley TM (2003) Ion Suppression in Mass Spectrometry. Clinical Chemistry 49 (7):1041–1044. 10.1373/49.7.1041 [PubMed: 12816898]
49. Taylor AJ, Dexter A, Bunch J (2018) Exploring Ion Suppression in Mass Spectrometry Imaging of a Heterogeneous Tissue. Analytical Chemistry 90 (9):5637–5645. 10.1021/acs.analchem.7b05005 [PubMed: 29461803]
50. Li G, Cao Q, Liu Y, DeLaney K, Tian Z, Moskovets E, Li L (2019) Characterizing and alleviating ion suppression effects in atmospheric pressure matrix-assisted laser desorption/ionization. Rapid Commun Mass Spectrom 33 (4):327–335. 10.1002/rcm.8358 [PubMed: 30430670]

51. Villarreal JC, Williams S, Egatz-Gomez A, Coleman P, Nedelkov D, Sierks MR, Ros A Alzheimer's disease specific markers detected with microfluidic MALDI mass spectrometry (MIMAS) In: 21st International Conference on Miniaturized Systems for Chemistry and Life Sciences, MicroTAS 2017, 2017. pp 1287–1288
52. Villarreal JC, Egatz-Gomez A, Liu J, Ros R, Coleman PD, Ros A Amyloid β analysis from microdissected brain cells using microfluidics and maldi mass spectrometry In: MicroTAS 2020 – 24th International Conference on Miniaturized Systems for Chemistry and Life Sciences, 2020. pp 711–712
53. Zenobi R, Knochenmuss R (1998) Ion formation in MALDI mass spectrometry. Mass Spectrom Rev 17 (5):337–366. 10.1002/(SICI)1098-2787(1998)17:5
54. Rechthaler J, Pittenauer E, Schaub TM, Allmaier G (2013) Detection of amine impurity and quality assessment of the MALDI matrix α-cyano-4-hydroxy-cinnamic acid for peptide analysis in the amol range. Journal of the American Society for Mass Spectrometry 24 (5):701–710. 10.1007/s13361-013-0614-0 [PubMed: 23595260]
55. Demeure K, Quinton L, Gabelica V, De Pauw E (2007) Rational selection of the optimum MALDI matrix for top-down proteomics by in-source decay. Anal Chem 79 (22):8678–8685. 10.1021/ac070849z [PubMed: 17939742]
56. Kussmann M, Nordhoff E, Rahbek-Nielsen H, Haebel S, Rossel-Larsen M, Jakobsen L, Gobom J, Mirgorodskaya E, Kroll-Kristensen A, Palm L, Roepstorff P (1997) Matrix-assisted Laser Desorption/Ionization Mass Spectrometry Sample Preparation Techniques Designed for Various Peptide and Protein Analytes. J Mass Spectrom 32 (6):593–601. 10.1002/(SICI)1096-9888(199706)32:6
57. Cohen SL, Chait BT (1996) Influence of matrix solution conditions on the MALDI-MS analysis of peptides and proteins. Anal Chem 68 (1):31–37. 10.1021/ac9507956 [PubMed: 8779435]
58. Ng HT, Fang A, Huang L, Li SFY (2002) Protein Microarrays on ITO Surfaces by a Direct Covalent Attachment Scheme. Langmuir 18 (16):6324–6329. 10.1021/la0255828
59. Tajima N, Takai M, Ishihara K (2011) Significance of Antibody Orientation Unraveled: Well-Oriented Antibodies Recorded High Binding Affinity. Anal Chem 83 (6):1969–1976. 10.1021/ac1026786 [PubMed: 21338074]
60. Trilling AK, Beekwilder J, Zuilhof H (2013) Antibody orientation on biosensor surfaces: a minireview. Analyst 138 (6):1619–1627. 10.1039/C2AN36787D [PubMed: 23337971]
61. Pei Z, Anderson H, Myrskog A, Dunér G, Ingemarsson B, Aastrup T (2010) Optimizing immobilization on two-dimensional carboxyl surface: pH dependence of antibody orientation and antigen binding capacity. Anal Biochem 398 (2):161–168. 10.1016/j.ab.2009.11.038 [PubMed: 19962366]
62. Glass NR, Tjeung R, Chan P, Yeo LY, Friend JR (2011) Organosilane deposition for microfluidic applications. Biomicrofluidics 5 (3):036501. 10.1063/1.3625605
63. Fiddes LK, Chan HKC, Lau B, Kumacheva E, Wheeler AR (2010) Durable, region-specific protein patterning in microfluidic channels. Biomaterials 31 (2):315–320. 10.1016/j.biomaterials.2009.09.040 [PubMed: 19800682]
64. Wang Y, Lai H-H, Bachman M, Sims CE, Li GP, Allbritton NL (2005) Covalent Micropatterning of Poly(dimethylsiloxane) by Photografting through a Mask. Anal Chem 77 (23):7539–7546. 10.1021/ac0509915 [PubMed: 16316160]
65. Sonker M, Parker EK, Nielsen AV, Sahore V, Woolley AT (2017) Electrokinetically operated microfluidic devices for integrated immunoaffinity monolith extraction and electrophoretic separation of preterm birth biomarkers. Analyst 143 (1):224–231. 10.1039/c7an01357d [PubMed: 29136068]
66. Barré FPY, Paine MRL, Flinders B, Trevitt AJ, Kelly PD, Ait-Belkacem R, Garcia JP, Creemers LB, Stauber J, Vreeken RJ, Cillero-Pastor B, Ellis SR, Heeren RMA (2019) Enhanced Sensitivity Using MALDI Imaging Coupled with Laser Postionization (MALDI-2) for Pharmaceutical Research. Anal Chem 91 (16):10840–10848. 10.1021/acs.analchem.9b02495 [PubMed: 31355633]
67. Zubair F (2021) MALDI mass Spectrometry based proteomics for drug discovery & development. Drug Discov Today 10.1016/j.ddtec.2021.09.002

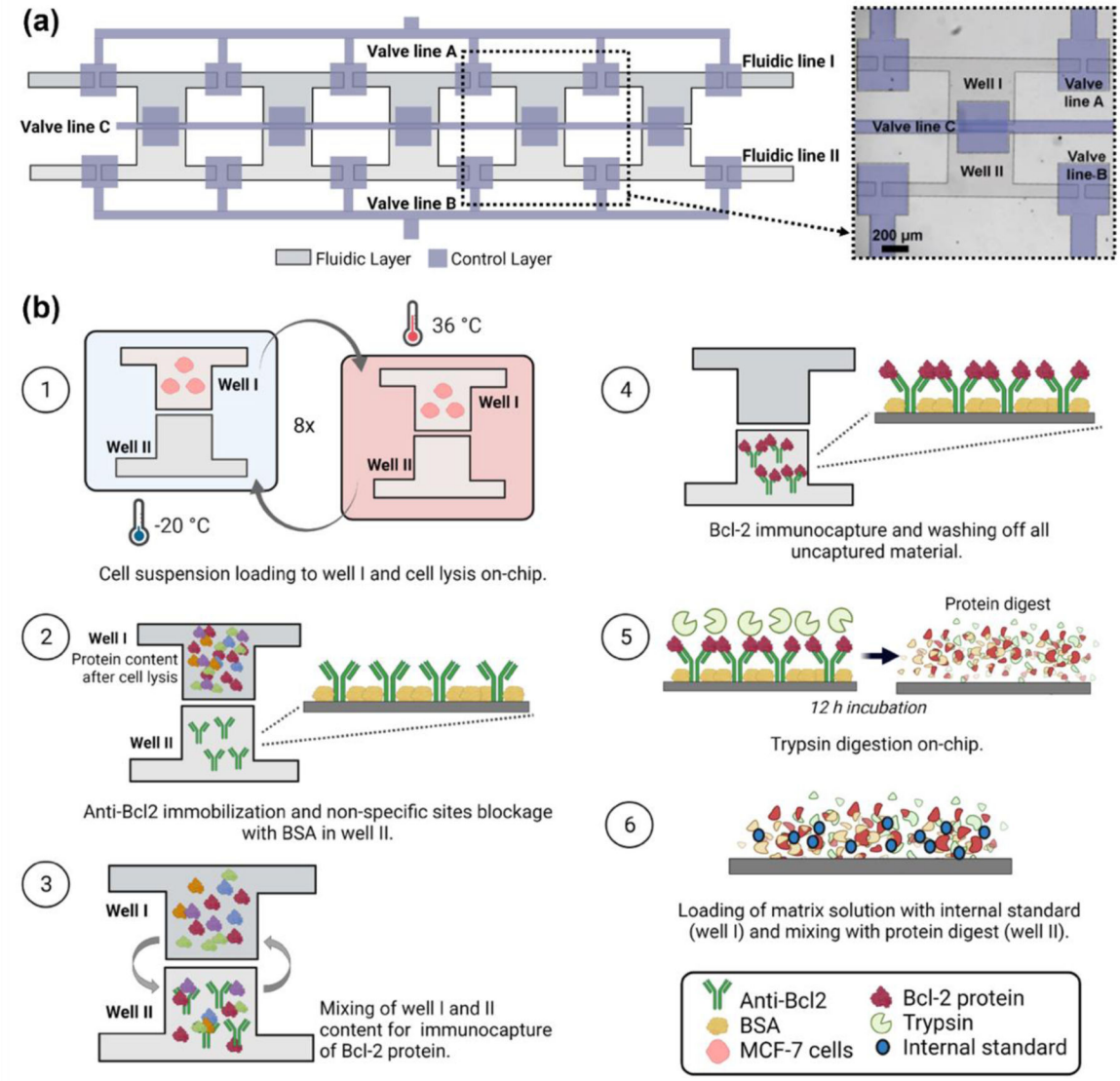

Fig. 1.

(a) Schematic of the device with 5 pairs of wells showing the fluidic wells and control valve layers. Inset: Bright-field microscopy image of a well pair with control layer (valves) highlighted in blue. (b) Workflow of MIMAS assay: (1) Loading of cell suspension and cell lysis by freezing and thawing cycles, (2) immobilization of anti-Bcl2 and blocking step, (3) mixing of well I and well II content, (4) immunocapture, (5) trypsin digestion, (6) addition of matrix solution and internal standard.

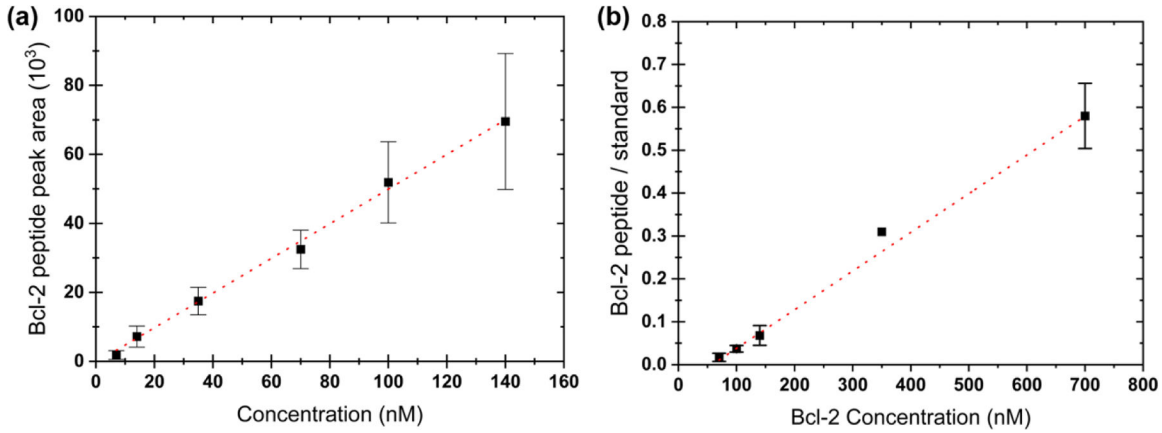

Fig. 2.

(a) Resulting Bcl-2 synthetic peptide (m/z 1210.6) peak area from MALDI-MS analysis at different concentrations (n=5) in the MIMAS device. (b) Resulting peak area ratio of Bcl-2 peptide FATVVEELFR and standard FATVVEEL(13C,15N)FR) with a fixed concentration of 1,400 nM for FATVVEEL(13C,15N)FR after the immunocapture and digestion on chip of Bcl-2 protein. Bcl-2 concentrations were varied in the MIMAS device. Error bars represent the standard deviation (n=3, except for 350 nM with n=1). Red dotted line represents the weighted linear regression with $R^2 = 0.99$ for (a) and $R^2 = 0.98$ for (b).

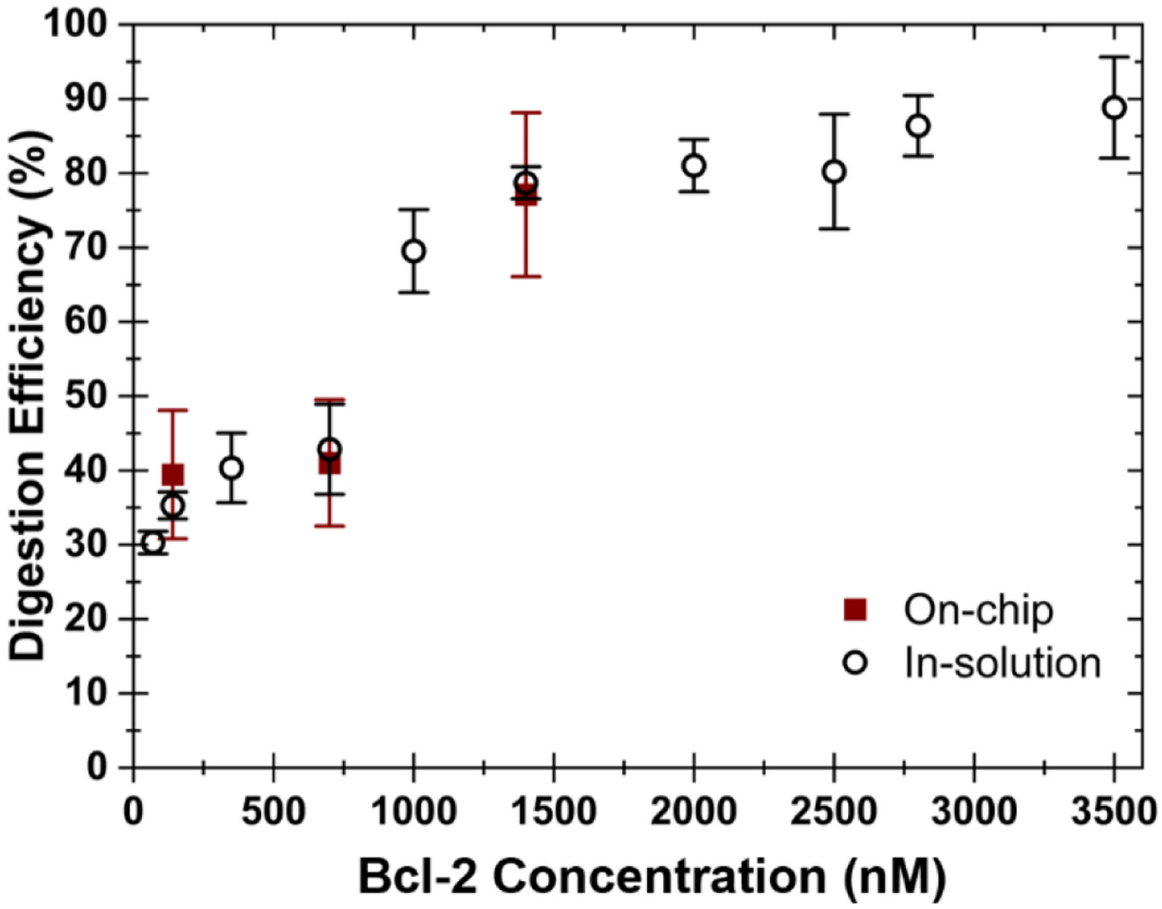

Fig. 3.

Digestion efficiency of Bcl-2 protein on-chip assessed with various concentrations in the 8.75 nL MIMAS well and in-solution with a fixed trypsin concentration (0.1 μg/μL). Internal standard FATVVEEL(13C,15N)FR was added to each condition at the same Bcl-2 protein concentration. The error bars represent the standard deviation (n = 8).

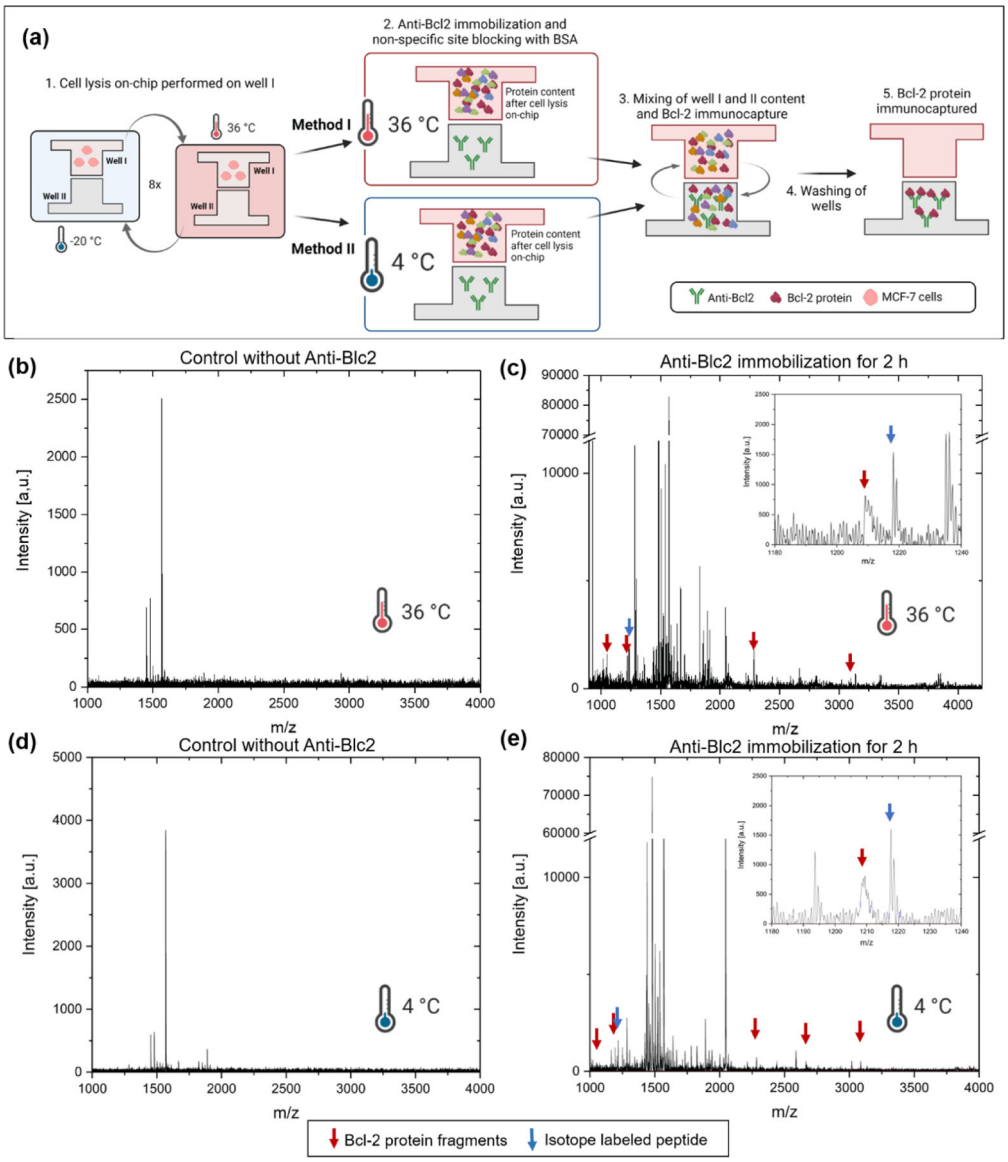

Fig. 4.

(a) Schematics of antibody immobilization with method I and II: incubation steps at 36 °C and at 4 °C, respectively. (b) Representative MS spectrum of control assay carried out with method I (36 °C). (c) Representative MS spectrum of the entire assay carried out with method I (36 °C) and an inset of the FATVVEELFR and FATVVEEL(13C,15N)FR used for quantification. (d) Representative MS spectrum of control assay carried out with method II (4 °C). (e) Representative MS spectrum of the entire assay carried out with method II (4 °C) and an inset of the FATVVEELFR and FATVVEEL(13C,15N)FR used for quantification.

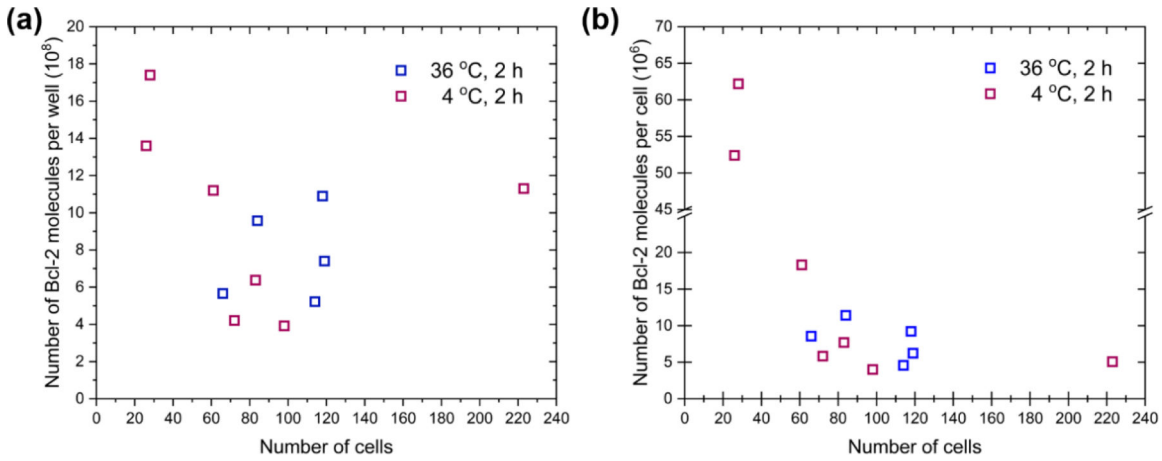

Fig. 5.

(a) Number of Bcl-2 molecules per well vs number of cells based on the Bcl-2 tryptic peptide m/z 1210.6 ratio to the isotope labeled peptide m/z 1217.6 for antibody immobilization at 36 °C for 2 h, and at 4 °C for 2 h. (b) Number of Bcl-2 molecules per cells vs number of cells based on the ratio of Bcl-2 tryptic peptide m/z 1210.6 to the isotope labeled peptide m/z 1217.6 for antibody immobilization at 36 °C for 2 h, and at 4 °C for 2 h. Some cases lack the presence of the Bcl-2 tryptic peptide used for quantification (m/z 1210.6), thus, an estimate number of molecules per well is not available for all the data points (less than ten data points are shown per specified temperature although ten wells were tested).

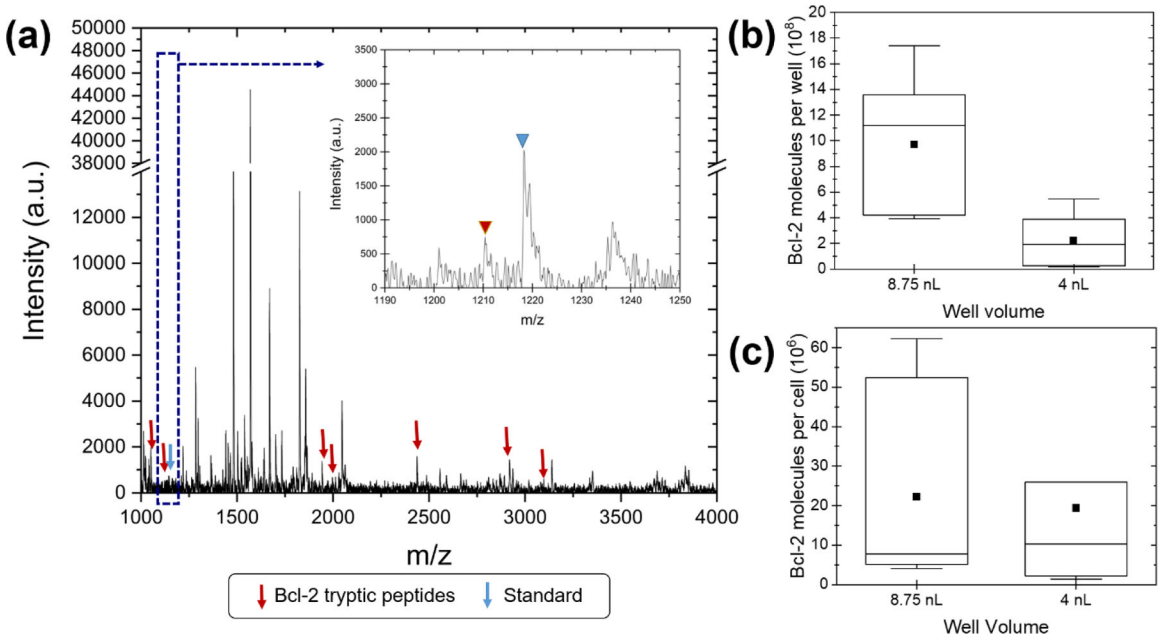

Fig. 6.

(a) Representative spectrum of the MIMAS assay performed using 300 × 300 μm wells, indicating the Bcl-2 protein tryptic peptides. Zoom-in of the spectrum indicating the Bcl-2 peptide m/z 1210.6 and isotope labeled peptide m/z 1217.6 used for quantification. (b) Box plot of the calculated number of Bcl-2 molecules per well based on the peak area ratio of the Bcl-2 tryptic peptide and the standard using the wells with volume of 8.75 nL and 4 nL. The average number of cells for wells with 8.75 nL is 89 ± 50 and for wells with 4 nL is 14 ± 4, (significantly different at $p = 0.012$). (c) Box plot of the estimated number of Bcl-2 molecules per cell for the experiments in wells with volume of 8.75 nL and 4 nL, which are not significantly different ($p = 0.979$). The box contains 5–95% of the data, the average is presented by ■, and the line in the box represents the median.